Blind fluorescence structured illumination microscopy: A new reconstruction strategy

Simon LABOUESSE[1], Marc ALLAIN[1], Jérôme IDIER[2], Sébastien BOURGUIGNON[2], Penghuan LIU[2], Anne SENTENAC[1]

[1]Aix-Marseille Université, CNRS, Centrale Marseille, Institut Fresnel UMR 7249, 13013 Marseille, France

[2]L'UNAM Université, École Centrale de Nantes, CNRS, IRCCyN, UMR 6597, 44321 Nantes, France

simon.labouesse@fresnel.fr, marc.allain@fresnel.fr, jerome.idier@irccyn.ec-nantes.fr
sebastien.bourguignon@irccyn.ec-nantes.fr, penghuan.liu@irccyn.ec-nantes.fr,
anne.sentenac@fresnel.fr

Résumé – Nous proposons dans cette communication un nouvel algorithme de reconstruction d'image super-résolue dédié à la microscopie à éclairements structurés *aveugle* (blind-SIM), c'est-à-dire sans connaissance préalable des illuminations ayant éclairé l'objet. Simple à programmer et d'un faible coût de calcul par itération, ce nouvel algorithme ouvre la voie vers l'imagerie 2D temps réel et 3D.

Abstract – In this communication, a fast reconstruction algorithm is proposed for fluorescence *blind* structured illumination microscopy (SIM) under the image positivity constraint. This new algorithm is by far simpler and faster then existing solutions, paving the way to 3D and/or real-time 2D reconstruction.

1 Introduction

Classical wide-field fluorescence microscopy aims at imaging the fluorescence density ρ emitted from a marked biological sample. In the linear regime, the recorded intensity is related to ρ *via* a simple convolution model [5]. If one proceeds to M distinct acquisitions, the dataset $\{y_m\}_{m=1}^M$ is given by

$$y_m = h \otimes (\rho \times I_m) + \varepsilon_m \qquad m = 1 \cdots M \qquad (1)$$

where $\otimes$ is the convolution operator, h is the point-spread function (PSF), I_m is the m-th illumination intensity pattern, and ε_m is a perturbation term accounting for (electronic) noise in the detection and model errors. The final resolution of the microscope is ultimately limited by the optical transfer function (OTF)[1] $\tilde{h}$, whose cutoff frequency is fixed by the emitted wavelength and by the numerical aperture of the microscope objective. The frequency limit is strict with uniform illuminations. However, structured illuminations can be used to shift high-frequency components of the object into the OTF support [7]. Such a strategy results in the standard *structured illumination microscopy* (SIM) that resorts to harmonic illumination patterns to achieve super-resolution reconstruction. Because SIM uses the illumination patterns as references, strong artifacts are induced if the patterns are not known with sufficient accuracy [9, 1]. From a practical viewpoint, such a condition is very stringent and restricts standard SIM to thin samples or to samples with small refraction indices [9]. The Blind-SIM strategy [9] has been proposed to tackle this problem, the principle being to retrieve the sample fluorescence density without the knowledge of the illumination patterns, thereby extending the potential of SIM. In addition, this strategy promotes the use of speckle illumination patterns instead of harmonic illumination patterns, the latter standard case being much more difficult to generate.

From the methodological viewpoint, Blind-SIM relies on the *simultaneous* reconstruction of the fluorescence density and of the illumination patterns. More precisely, in [9], joint reconstruction is achieved through the iterative resolution of a constrained least-squares problem based on conjugate gradient iterations. However, the computational time of such a scheme (as reported in [9, Supplementary material]) clearly restricts the applicability of the resulting blind-SIM strategy. In this paper, the implementation issues of *Blind*-SIM are revisited and drastically simplified: a much improved implementation is proposed, with an execution time decreased by several orders of magnitude. Moreover, it can be highly parallelized, opening the way to real-time blind-SIM reconstructions.

[1]In the sequel, the notation $\tilde{\cdot}$ stands for the Fourier Transform (or the Discrete Fourier Transform if a vector is considered).

2 Blind-SIM reformulation

In the sequel, we focus on a discretized formulation of the observation model (1). Solving the two-dimensional (2D) Blind-SIM reconstruction problem is equivalent to finding a *joint* solution $(\widehat{\boldsymbol{\rho}}, \{\widehat{\boldsymbol{I}}_m\}_{m=1}^M)$ to the following constrained minimisation problem [9]:

$$\min_{\boldsymbol{\rho}, \{\boldsymbol{I}_m\}} \quad \sum_{m=1}^M \|\boldsymbol{y}_m - \boldsymbol{H}\mathrm{diag}(\boldsymbol{\rho})\,\boldsymbol{I}_m\|^2 \tag{2a}$$

$$\text{subject to} \quad \sum_m \boldsymbol{I}_m = M \times \boldsymbol{I}_0 \tag{2b}$$

$$\rho_n \geq 0, \quad I_{m;n} \geq 0, \qquad \forall m, n \tag{2c}$$

with $\boldsymbol{H} \in \mathbb{R}^{N\times N}$ the 2D convolution matrix built from the discretized PSF. We also denote $\boldsymbol{\rho} = \mathrm{Vect}\,(\rho_n) \in \mathbb{R}^N$ the discretized fluorescence density, $\boldsymbol{y}_m = \mathrm{Vect}\,(y_{m;n}) \in \mathbb{R}^N$ the m-th recorded image, and $\boldsymbol{I}_m = \mathrm{Vect}\,(I_{m;n}) \in \mathbb{R}^N$ the m-th illumination with spatial mean $\boldsymbol{I}_0 = \mathrm{Vect}\,(I_{0;n}) \in \mathbb{R}^N$. Let us remark that (2) is a *biquadratic* problem. Block coordinate descent alternating between the object and the illuminations could be a possible minimisation strategy, relying on sequentially solving $M+1$ quadratic programming problems. In [9], a more efficient but more complex scheme is proposed. However, the minimisation problem (2) has a very specific structure, yielding a fast and simple strategy, as shown below.

Let us first consider problem (2) without the equality constraint (2b). It then becomes equivalent to M quadratic minimisation problems

$$\min_{\boldsymbol{q}_m} \|\boldsymbol{y}_m - \boldsymbol{H}\boldsymbol{q}_m\|^2 \tag{3a}$$

$$\text{subject to} \quad \boldsymbol{q}_m \geq 0 \tag{3b}$$

where

$$\forall m, \qquad \boldsymbol{q}_m \stackrel{\text{def}}{=} \mathrm{diag}(\boldsymbol{\rho}) \times \boldsymbol{I}_m.$$

with $\mathrm{diag}(\boldsymbol{\rho})$ the diagonal matrix with vector ρ on the diagonal. Each minimisation problem (3) can be separately solved in a simple and efficient way (see Sec. 4), hence providing a set of global minimizers $\{\widehat{\boldsymbol{q}}_m\}_{m=1}^M$. Although the latter set corresponds to an infinite number of solutions $(\widehat{\boldsymbol{\rho}}, \{\widehat{\boldsymbol{I}}_m\}_{m=1}^M)$, the equality constraint in (2b) defines a unique solution such that $\mathrm{diag}(\widehat{\boldsymbol{\rho}}) \times \widehat{\boldsymbol{I}}_m = \widehat{\boldsymbol{q}}_m$ for all m:

$$\widehat{\boldsymbol{\rho}} = \mathrm{diag}(\boldsymbol{I}_0)^{-1}\,\overline{\boldsymbol{q}} \tag{4a}$$

$$\forall m \qquad \widehat{\boldsymbol{I}}_m = \mathrm{diag}(\widehat{\boldsymbol{\rho}})^{-1}\,\widehat{\boldsymbol{q}}_m \tag{4b}$$

where

$$\overline{\boldsymbol{q}} \stackrel{\text{def}}{=} \tfrac{1}{M}\textstyle\sum_m \widehat{\boldsymbol{q}}_m = \mathrm{diag}(\widehat{\boldsymbol{\rho}})\,\tfrac{1}{M}\textstyle\sum_m \widehat{\boldsymbol{I}}_m = \mathrm{diag}(\widehat{\boldsymbol{\rho}})\,\boldsymbol{I}_0.$$

Moreover, the following implications hold:

$$I_{0;n} > 0, \quad \text{and} \quad \widehat{q}_{m;n} > 0,$$
$$\implies \qquad \widehat{I}_{m,n} \geq 0 \quad \text{and} \quad \widehat{\rho}_n \geq 0 \qquad \forall n, m.$$

Because we are dealing with intensity patterns, the condition $\boldsymbol{I}_0 \geq 0$ is always met, hence ensuring the positivity of both the density and the illumination estimates. We also note that a solution (4) exists as long as $I_{0;n} \neq 0$ and $\widehat{\rho}_n \neq 0$, $\forall n$. The first condition is met if the sample is illuminated everywhere, which is an obvious minimal requirement. For any pixel sample such that $\widehat{\rho}_n = 0$, the corresponding illumination $\widehat{I}_{m;n}$ is not defined; this is not a problem as long as the fluorescence density $\boldsymbol{\rho}$ is the only quantity of interest.

3 Super-resolution in Blind-SIM

Whereas the mechanism that conveys super-resolution with *known* structured illuminations is well understood (see [6] for instance), the super-resolution capacity of blind-SIM has not been characterized yet. It can be made clear, however, that the positivity constraint (2c) plays a central role in this regard. Let $\boldsymbol{H}^+$ be the *pseudo-inverse* of $\boldsymbol{H}$ [4, Sec. 5.5.4]. Then, any solution to the problem without positivity constraints (2a)-(2b) reads

$$\widehat{\boldsymbol{\rho}} = \mathrm{diag}(\boldsymbol{I}_0)^{-1}(\boldsymbol{H}^+\overline{\boldsymbol{y}} + \overline{\boldsymbol{q}}^{\perp}) \tag{5a}$$

$$\widehat{\boldsymbol{I}}_m = \mathrm{diag}(\widehat{\boldsymbol{\rho}})^{-1}(\boldsymbol{H}^+\boldsymbol{y}_m + \boldsymbol{q}_m^{\perp}), \tag{5b}$$

with $\overline{\boldsymbol{y}} = \frac{1}{M}\sum_m \boldsymbol{y}_m$, and $\overline{\boldsymbol{q}}^{\perp} = \frac{1}{M}\sum_m \boldsymbol{q}_m^{\perp}$ where $\boldsymbol{q}_m^{\perp}$ is an arbitrary element of the kernel of $\boldsymbol{H}$, *i.e.* an arbitrary high-frequency component. Hence, the formulation (2a)-(2b) has no capacity to discriminate the correct high frequency components, which means that it has no super-resolution capacity. Under the positivity constraint (2c), we thus expect that the super-resolution capacity of blind-SIM depends on the fact that each illumination pattern $\boldsymbol{I}_m$ activates the positivity constraint on $\boldsymbol{q}_m$ in a frequent manner. Such adequate illumination patterns can be easily generated as speckle images, as proposed by [9]. In contrast, standard SIM rests upon the amplitude modulation of the object, *i.e.*, it only needs illumination patterns with broad-band spectra.

Let us stress that each problem (3) is convex quadratic, and thus admits only global solutions, which in turn provide global solutions to problem (2), when recombined according to (4a)-(4b). On the other hand, problems (3) may not admit unique solutions, since $\|\boldsymbol{y}_m - \boldsymbol{H}\boldsymbol{q}_m\|^2$ is not strictly convex in $\boldsymbol{q}_m$. A simple way to enforce unicity is to slightly modify (3) by adding a strictly convex penalization term. We are thus led to solving

$$\min_{\boldsymbol{q}_m \geq 0} \textstyle\sum_{m=1}^M \mathcal{J}_m(\boldsymbol{q}_m) \tag{6a}$$

with

$$\mathcal{J}_m(\boldsymbol{q}) \stackrel{\text{def}}{=} \|\boldsymbol{y}_m - \boldsymbol{H}\boldsymbol{q}\|^2 + \varphi(\boldsymbol{q}). \tag{6b}$$

Another advantage of such an approach is that φ can be chosen so that robustness to the noise is granted and/or some expected features in the solution are enforced. In particular, the analysis conveyed above suggests that favoring sparsity in each $\boldsymbol{q}_m$ is suited since speckle or periodic illumination patterns tend to frequently cancel or

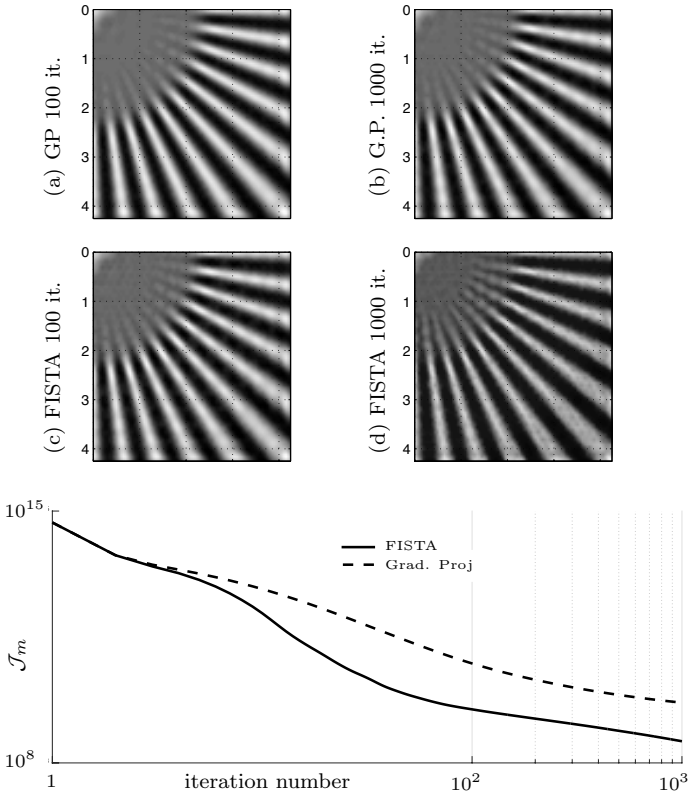

FIG. 1: [Top] Harmonic blind-SIM reconstruction of the fluorescence pattern achieved by the minimization of the penalized criterion (6) with 100 or 1000 projected-gradient (a,b) or FISTA (c,d) iterations. [Bottom] Evolution of the criterion (6) as a function of the iteration number for the projected-gradient (plain) and the FISTA (dot) algorithm. All these simulations were performed with ($\alpha = 6.10^4, s = 150$). The reconstruction (d) corresponds to the one that is shown in Fig. 2-(d).

nearly cancel the product images $\boldsymbol{q}_m$, i.e., an appropriate modeling for $\boldsymbol{q}_m$ is the "near black object" as introduced in [3]. Following this line, we found that enforcing sparsity *via* the standard separable ℓ_1 penalty provides super-resolved reconstructions at high signal-to-noise ratio (SNR). For moderate SNR values, though, we have found more appropriate to consider an ℓ_{21} separable penalty such as [8]:

$$\varphi(\boldsymbol{q}; \alpha, s) \stackrel{\text{def}}{=} \alpha \sum_n \sqrt{q_n^2 + s^2} \tag{7}$$

where the parameters $\alpha \geq 0$ and $s > 0$ need to be adjusted.

4 Proposed blind-SIM approach

The criterion (6b) [equipped with (7)] enjoys good structural properties: it is a smooth, strictly convex function with a Lipschitz continuous gradient. Such properties ensure that the constrained optimization problem (6) can be solved by mean of simple projected-gradient iterations. Here, we consider the accelerated version FISTA [2]. Let $\mathcal{P}_+$ be the projector over the positive orthant, and let $\boldsymbol{q}_m^{(0)} \in \mathbb{R}_+^N$ and $\boldsymbol{\omega}^{(0)} = \boldsymbol{q}_m^{(0)}$ be the initial solution. For the m-th subproblem, the iterations read

$$\boldsymbol{q}_m^{(k+1)} \longleftarrow \mathcal{P}_+ \left(\boldsymbol{\omega}^{(k)} - \gamma^{(k)} \nabla \mathcal{J}_m(\boldsymbol{\omega}^{(k)}) \right) \tag{8a}$$

$$\boldsymbol{\omega}^{(k+1)} \longleftarrow \boldsymbol{q}_m^{(k+1)} + \tfrac{k-1}{k+2} \left(\boldsymbol{q}_m^{(k+1)} - \boldsymbol{q}_m^{(k)} \right) \tag{8b}$$

where the step-size is chosen such that $\epsilon < \gamma^{(k)} < 2/L - \epsilon$ to ensure global convergence, L being the Lipschitz constant that reads

$$L = 2\lambda_{\max}(\boldsymbol{H}^t \boldsymbol{H}) + \alpha s^{-1}. \tag{9}$$

where $\lambda_{\max}(\boldsymbol{A})$ denotes the highest eigenvalue of the matrix $\boldsymbol{A} \in \mathbb{R}^{N \times N}$. The asymptotic convergence achieved by (8) is $O(1/k^2)$, which is a substantial gain compared to the $O(1/k)$ rate of the standard gradient-projected iteration [2]. Figure 1 gives an illustration of this accelerated convergence with one of the reconstructions discussed in the next paragraph.

For illustrative purposes, the numerical blind-SIM experiment presented in [9] is now considered. The ground-truth consists in the 2D 'star-like' fluorescence pattern depicted in Fig. 2(a). The M collected images are simulated following (1) with the PSF h given by the Airy pattern that reads [in polar (r, θ) coordinates]

$$h(r, \theta) = \left(\frac{J_1(r\, k_0\, \mathrm{NA})}{k_0\, r} \right)^2 \frac{k_0^2}{\pi} \tag{10}$$

where J_1 is the first order Bessel function of the first kind, NA is the objective numerical aperture set to 1.49, and $k_0 = 2\pi/\lambda$ is the free-space wavenumber with λ the emission and the excitation wavelengths. The image sampling step for all the simulations is set to $\lambda/20$. The illumination set $\{\boldsymbol{I}_m\}_{m=1}^M$ consists either in $M = 9$ *periodic patterns* with spatial frequency equal to $2/\lambda$, or in $M = 100$ *speckle patterns* with spatial correlation given by (10). Finally, the collected images are corrupted with Gaussian noise. The standard deviation for a single acquisition was chosen so that the total SNR is 30 dB for both the periodic and speckle experiments. The subproblem hyperparameters were set to ($\alpha = 6.10^4, s = 150$) for the periodic and the speckle illuminations. The initial-guess and the step-size were set to $\boldsymbol{q}_m^{(0)} = \boldsymbol{0}$ and $\gamma^{(k)} = 0.85 \times 2/L$ ($\forall k$), respectively. The reconstruction of Fig. 2(c)-(d) clearly shows a super-resolution effect similar to the one obtained in [9]. In particular, this simulation corroborates the empirical statement that $M \approx 10$ harmonic illuminations and $M \approx 100$ speckle illuminations produce almost equivalent super-resolved reconstructions. Obviously, imaging with random speckle patterns remains an attractive strategy since it is achieved with a very simple experimental setup, see [9] for details.

The interest of the proposed strategy is that the iterations (8) can be easily implemented, at a low computa-

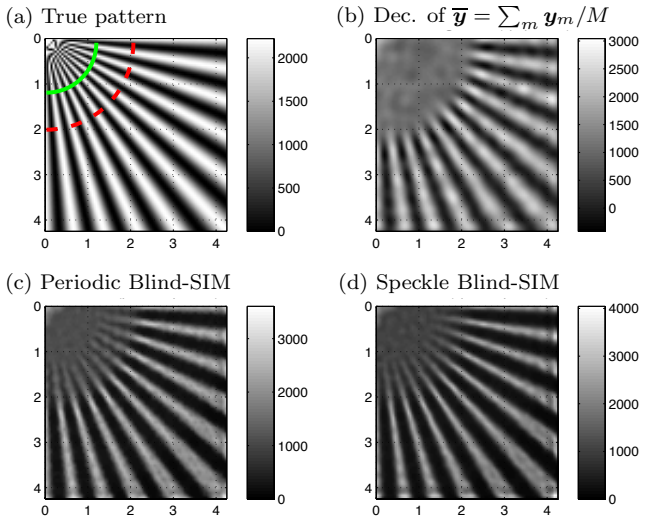

FIG. 2: Right lower quadrant of the (200 × 200 pixels) true fluorescence pattern (a), deconvolution of the averaged speckle patterns (b), and blind-SIM reconstructions with $M = 9$ periodic (c) and $M = 100$ speckle patterns (d). The graduations are in λ. The dashed (resp. solid) lines in (a) corresponds to the spatial frequencies transmitted by (resp. twice) the OTF support.

tional cost; for instance, the speckle and periodic blind-SIM reconstruction shown in Fig. 2 were respectively obtained in about 100 and 10 seconds with a standard Matlab implementation on a regular laptop computer. On the other hand, let us remark that our strategy requires an explicit tuning of the parameters α and s, whereas the constrained conjugate gradient approach proposed in [9] is regularized through the number of iterates. Since adequate values of α and s will depend mostly on experimental parameters (PSF, noise and signal levels, number of views), a simple calibration step seems possible.

5 Conclusion

The reformulation presented in Sec. 2 unveiled some of the super resolution properties of the joint reconstruction problem introduced in [9]. We feel however that this blind-SIM approach deserves further investigations, both from the theoretical and the experimental viewpoints. In particular, the *joint* reconstruction approach considered here produces some systematic errors (*i.e.*, bias) that should be evaluated. Indeed, we are currently exploring a *marginal strategy* aiming at estimating $\boldsymbol{\rho}$ *only*, which could be preferable from the statistical viewpoint. Finally, some experimental datasets should be considered shortly. One expected difficulty arising in the processing of such real data sets is the strong background induced in the focal plane by the out-of-focus light. This phenomenon prevents the local extinction of the excitation intensity, hence destroying the expected super-resolution in blind-SIM. The modeling of this background with a very smooth function is possible [10] and will be considered. A different approach would be to solve the reconstruction problem in its 3D structure, which is numerically challenging, but remains a mandatory step to achieve 3D reconstructions.

Acknowledgement. The GDR ISIS is acknowledged for the partial funding of this work.

References

[1] R. Ayuk, H. Giovannini, A. Jost, E. Mudry, J. Girard, T. Mangeat, N. Sandeau, R. Heintzmann, K. Wicker, K. Belkebir, and A. Sentenac. Structured illumination fluorescence microscopy with distorted excitations using a filtered blind-simalgorithm. *Optics Letters*, 38(22):4723–4726, Nov 2013.

[2] A. Beck and M. Teboulle. A fast iterative shrinkage-thresholding algorithm for linear inverse problems. *SIAM J. Imaging Sciences*, 2(1):183–202, 2009.

[3] D. L. Donoho, A. M. Johnstone, J. C. Hoche, and A. S. Stern. Maximum entropy and the nearly black object. *Journal of the Royal Statistical Society*, 198:41–81, 1992.

[4] G. H. Golub and C. H. Van Loan. *Matrix computation*. The Johns Hopkins University Press, Baltimore, 3rd ed. edition, 1996.

[5] J.W. Goodman. *Introduction to Fourier Optics*. Roberts & Company Publishers, 2005.

[6] M. G. L. Gustafsson. Surpassing the lateral resolution limit by a factor of two using structured illumination microscopy. *Journal of Microscopy*, 2000.

[7] R. Heintzmann and C. Cremer. Laterally modulated excitation microscopy: improvement of resolution by using a diffraction grating. In *Proc. SPIE, Optical Biopsies and Microscopic Techniques III*, pages 185–196, 1999.

[8] S. Labouesse, M. Allain, J. Idier, S. Bourguignon, P. Liu, and A. Sentenac. Super-resolved reconstruction in a blind-SIM strategy. Research report, Institut Fresnel, march 2015.

[9] E. Mudry, K. Belkebir, J. Savatier, E. Le Moal, C. Nicoletti, M. Allain, and A. Sentenac. Structured illumination microscopy using unknown speckle patterns. *Nature Photonics*, 6:312–315, 2012.

[10] F. Orieux, E. Sepulveda, V. Loriette, B. Dubertret, and J.-C. Olivo-Martin. Bayesian estimation for optimized structured illumination microscopy. *IEEE Transactions on image processing*, 21(2):601–614, 2012.